

# K<sub>2</sub>SrIn<sub>7</sub>: An Electron-Deficient Indium Network Structure That Reflects Limitations of Cation Accommodation. Synthesis, Structure, and Bonding

Lisheng Chi and John D. Corbett\*

Ames Laboratory-DOE<sup>1</sup> and Department of Chemistry, Iowa State University, Ames, Iowa 50011

Received January 5, 2001

A new phase in the K–Sr–In system was discovered following direct fusion of the neat elements in a niobium tube at 900 °C and equilibration at 700 °C for 5 days. Single-crystal X-ray diffraction analysis reveals that K<sub>2</sub>SrIn<sub>7</sub> crystallizes in an orthorhombic system, space group *Cmcm*, *Z* = 4, *a* = 5.0455(5) Å, *b* = 11.960(2) Å, *c* = 19.762(4) Å. The structure contains a three-dimensional In network built of sheets of condensed pentagonal prismatic columns interbonded along  $\vec{c}$ . Two rather different types of channels are separately occupied by K and Sr atoms, the latter centered in 15-atom indium polyhedra. Band structure calculations and resistivity and susceptibility measurements indicate that the compound is metallic and diamagnetic. The one-electron deficiency in the valence band per formula unit brought on by the limited cation count is analyzed in terms of the character of the bonding, some of that from multicenter In bonding falling above *E<sub>F</sub>*.

## Introduction

Inorganic solid state chemistry must frequently confront both opportunities and challenges because, first, it is often quite difficult to predict the composition and crystal structure of any new stable compound and, second, these results often pertain to unprecedented and often conflicting factors. Therefore, exploratory synthesis remains a never ending, and often very exciting, endeavor. The presence of mixed cations differing in size, charge, and, sometimes, electronic states usually results in a quite different construction and connectivity than that with a single cation type. This is particularly true when polyanions are involved because the bonding also is governed by good packing and maximal Coulomb energy of the ion pairs. Thus, a considerable variety of potential clusters may be hidden from view in binary systems if the total energy of a pertinent phase cannot be maximized relative to alternative phases. In recent years, we have discovered a large number of new ternary triel and tetrel compounds through size tuning with mixed cations.<sup>2–4</sup> For instance, mixed cations in Ca<sub>6.2</sub>Mg<sub>3.8</sub>Sn<sub>7</sub><sup>5</sup> uniquely stabilize a phase that does not exist with only calcium cations, whereas only the compositions Na<sub>4</sub>A<sub>6</sub>Tl<sub>13</sub> (A = K, Rb, Cs) and Na<sub>3</sub>K<sub>8</sub>Tl<sub>13</sub> among alkali metal compounds evidently contain the isolated, centered Tl<sub>13</sub><sup>10–</sup> and Tl<sub>13</sub><sup>11–</sup> icosahedra, respectively.<sup>6</sup> The role of sodium in these is decisive, and the ion packing with the former cluster is particularly favorable even though it means that only the open shell cluster is obtained in this bcc version.

In general, the environments of the discrete ion-solvated cluster anions consist of cations that cap cluster faces or bridge

edges or are positioned exo at vertexes, the strongest interactions naturally being found with the shorter-ranged face-capping sites, as in Na<sub>23</sub>K<sub>9</sub>Tl<sub>15.33</sub>,<sup>7</sup> Na<sub>2</sub>K<sub>21</sub>Tl<sub>19</sub>,<sup>8</sup> and A<sub>3</sub>Na<sub>26</sub>In<sub>48</sub> (A = K, Rb, Cs).<sup>9</sup> A series of three closely related structures is obtained when further potassium substitutes in the last phase.<sup>10–12</sup> Even the proportions of mixed cations plays a vital role in the formation of certain phases.

Our recent explorations of the relatively unknown alkaline-earth-metal–indide systems have revealed a greater dominance of indium network phases than in alkali metal systems, as would be expected with the smaller proportion of cations necessary to achieve approximately the same electron count (VEC) per indium in the anionic portion. With SrIn<sub>4</sub><sup>13</sup> and Sr<sub>3</sub>In<sub>5</sub>,<sup>14</sup> it becomes clear that good accommodation of these dipositive cations is a substantial factor in the nature of the network substructure of the indide that is generated. Here we demonstrate in the formation of a new phase K<sub>2</sub>SrIn<sub>7</sub> the effects in yet another 3-D indide network of the need to provide good sites for mixed cations of different sizes and, particularly, charges.

## Experimental Section

**Synthesis.** The general reaction techniques have been described elsewhere.<sup>15–17</sup> The elements utilized, K (99.95%), Sr (99.9%), and In (5–9's) were all from Alfa-Aesar. All materials were handled in N<sub>2</sub>- or He-filled gloveboxes with moisture levels less than 0.1 ppm by volume. Before weighing, the surfaces of potassium, strontium, and indium were cut clean with a scalpel. An exploratory reaction with K:Sr:In proportions of 4:2:11 was loaded in a glovebox into a niobium tube welded at one end, and the second end was tightly crimped and

(1) This research was supported by the Office of Basic Energy Sciences, Materials Sciences Division, U.S. Department of Energy. Ames Laboratory is operated for DOE by Iowa State University under Contract No. W-7405-Eng-82.

(2) Corbett, J. D. In *Chemistry, Structure and Bonding of Zintl Phases and Ions*; Kauzlarich, S. M., Ed.; VCH Publishers: New York, 1996; Chapter 4.

(3) Corbett, J. D. *Angew. Chem., Int. Ed.* **2000**, *39*, 670.

(4) Corbett, J. D. *Inorg. Chem.* **2000**, *39*, 5178.

(5) Ganguli, A. K.; Corbett, J. D.; Köckerling, M. *J. Am. Chem. Soc.* **1998**, *120*, 1223.

(6) Dong, Z.-C.; Corbett, J. D. *J. Am. Chem. Soc.* **1995**, *117*, 6447.

(7) Dong, Z.-C.; Corbett, J. D. *Inorg. Chem.* **1996**, *35*, 3107.

(8) Dong, Z.-C.; Corbett, J. D. *J. Am. Chem. Soc.* **1994**, *116*, 3429.

(9) Sevov, S. C.; Corbett, J. D. *Inorg. Chem.* **1993**, *329*, 1612.

(10) Frank-Cordier, U.; Cordier, G.; Schäfer, H. *Z. Naturforsch.* **1982**, *37B*, 119.

(11) Ling, R. G.; Belin, C. *Acta Crystallogr.* **1982**, *38B*, 1101.

(12) Cordier, G.; Müller, V. *Z. Kristallogr.* **1991**, *198*, 302.

(13) Seo, D.-K.; Corbett, J. D. *J. Am. Chem. Soc.* **2000**, *122*, 9621.

(14) Seo, D.-K.; Corbett, J. D. *J. Am. Chem. Soc.*, in press.

(15) Sevov, S. C.; Corbett, J. D. *Inorg. Chem.* **1992**, *31*, 1895.

(16) Dong, Z.-C.; Corbett, J. D. *J. Cluster Sci.* **1995**, *6*, 187.

(17) Kaskel, S.; Corbett, J. D. *Inorg. Chem.* **2000**, *39*, 3086.

welded under an Ar atmosphere. The container was sealed in a fused-silica ampule under high vacuum ( $\sim 10^{-5}$  Torr) after baking. The mixture was initially heated to 900 °C for 24 h (the highest melting points in the K–In and Sr–In systems are 478 and 930 °C, respectively<sup>18</sup>), cooled to 700 °C at 30°/h, equilibrated at that temperature for 5 days, and then cooled to room temperature at 10°/h. The product was a grayish (reflective black) matrix in appearance with some shiny irregular crystals. The accurate phase composition was first established by single-crystal X-ray diffraction analysis. In addition, a later reaction with the indicated stoichiometry was run at 1000 °C for 6 h, annealed at 600 °C for 500 h, and then cooled to room temperature at 2°/h. The title phase was obtained in  $\geq 90\%$  yield according to its Guinier powder pattern, mixed with  $\leq 10\%$  of an unknown phase. On the other hand, the composition that would correspond to the valence-precise structure, K<sub>2</sub>SrIn<sub>7</sub>, did not produce any of the new compound, rather mainly SrIn<sub>2</sub>. Although a number of other reactions were run in this ternary system (spanning compositions of 2:1:5 to 2:4:11), only a couple of these produced the compound reported here. There does appear to be another indium-poorer phase. The Na–Sr–In system seems to contain only binary products.

**Structure Determination.** A few irregular crystals were picked from the products of the first reaction in a N<sub>2</sub>-filled crystal box, sealed in thin-walled capillaries, and checked by Laue and Weissenberg photographs for their singularity. Diffraction data from a  $\sim 0.1 \times 0.15 \times 0.45$  mm crystal were collected on a Rigaku AFC6R diffractometer at room temperature with the aid of graphite-monochromated Mo K $\alpha$  radiation. The initial cell parameters and an orientation matrix for data collection were obtained from a least-squares refinement of the setting angles of 25 reflections with a  $2\theta$  range of 22° to 50°. The Laue check indicated an *mmm* class. Two octants of data were collected with  $2\theta$ – $\omega$  scans at a rate of 16°/min and a scan width of  $0.84 + 0.34 \tan \theta$ °. The intensities of three standard reflections measured after collection of every 150 reflections remained essentially constant throughout data collection. A total of 1923 reflections was measured with a maximum  $2\theta$  value of 60°, of which 614 were independent, observed ( $I \geq 2\sigma(I)$ ), and used for structure solution and refinement.

The TEXSAN<sup>19</sup> program package was used for data processing. The raw data were corrected for Lorentz and polarization effects and for absorption empirically with the aid of three  $\psi$  scans ( $\mu = 183.9 \text{ cm}^{-1}$ ). The systematic observation conditions  $hkl$ ,  $h + k = 2n$ ;  $h0l$ ,  $h, l = 2n$ , indicated the orthorhombic space group *Cmcm* or *Cmc2<sub>1</sub>*. The Wilson plot clearly shows an centrosymmetric distribution associated with intensity statistics ( $|E^2 - 1| = 0.986$ ), and therefore the correct space group *Cmcm* was chosen for the initial trials. Seventy percent of the possible reflections were observed.

The structure was solved by direct methods and refined by full-matrix least squares on  $F^2$  for all data. The first step revealed five positions, the first four of which were assigned to In atoms and the fifth to Sr according to the distances around each. The subsequent difference Fourier synthesis contained only one significant peak which was reasonably assigned to K. After isotropic refinement of all positions, the  $R$  value was 5.08%, and the highest residual electron density peak was  $4.4 \text{ e}/\text{\AA}^3$ . After a secondary-extinction correction was applied, the final anisotropic refinement converged at  $R1 = 4.38\%$ ,  $wR2 = 10.17\%$ , and  $\text{GOF} = 1.022$  for 34 variables. The maximum and minimum peaks in the final difference Fourier map were  $3.708 \text{ e}/\text{\AA}^{-3}$  ( $0.96 \text{ \AA}$  from Sr) and  $-2.974 \text{ e}/\text{\AA}^{-3}$ , respectively. All calculations were performed using the SHELXTL<sup>20</sup> program package.

Some crystallographic and refinement details are listed in Table 1. Table 2 gives the atomic positional and isotropic displacement parameters, while Table 3 has the important bond distances. The more accurate Guinier-derived lattice dimensions were used for these calculations. More detailed crystallographic data and the anisotropic displacement parameters are contained in the Supporting Information. These and the structure factor data are also available from J.D.C.

**Table 1.** Some Crystal and Structure Refinement Data for K<sub>2</sub>SrIn<sub>7</sub>

fw	969.56
system, space group, $Z$	orthorhombic, <i>Cmcm</i> (No. 63), 4
unit cell dimensions <sup>a</sup> ( $\text{\AA}$ , $\text{\AA}^3$ )	
<i>a</i>	5.0455(5)
<i>b</i>	11.960(2)
<i>c</i>	19.762(4)
<i>V</i>	1192.5(2)
$d_{\text{calcd}}$ ( $\text{Mg}/\text{m}^3$ )	5.412
$\mu$ ( $\text{cm}^{-1}$ )	183.92
final indices <sup>b</sup> [ $I > 2\sigma(I)$ ]	
R1	0.0438
wR2	0.1017

<sup>a</sup> Refined from Guinier data with Si as internal standard,  $\lambda = 1.540562 \text{ \AA}$ , 23 °C. <sup>b</sup>  $R1 = \sum ||F_o| - |F_c|| / \sum |F_o|$ ;  $wR2 = [\sum w(|F_o|^2 - |F_c|^2)^2 / \sum w(F_o^2)]^{1/2}$ .

**Table 2.** Atomic Coordinates<sup>a</sup> ( $\times 10^4$ ) and Isotropic Equivalent Displacement Parameters ( $\text{\AA}^2 \times 10^3$ ) for K<sub>2</sub>SrIn<sub>7</sub>

	<i>y</i>	<i>z</i>	$U(\text{eq})^b$
In1	0441(1)	7500	18(1)
In2	4580(1)	5719(1)	16(1)
In3	-1221(1)	6298(1)	17(1)
In4	6401(1)	6747(1)	18(1)
Sr	3414(2)	7500	17(1)
K	1605(3)	5523(2)	20(1)

<sup>a</sup>  $x = 0$ . <sup>b</sup>  $U(\text{eq})$  is defined as one-third of the trace of the orthogonalized  $U_{ij}$  tensor.

**Table 3.** Bond Lengths in K<sub>2</sub>SrIn<sub>7</sub> ( $< 4.0 \text{ \AA}$ )

In1–In3	$3.095(2) \times 2$	In3–K	3.623(4)
In1–In4	$3.144(1) \times 4$	I3–K	3.707(4)
In2–In2	$3.011(2)$	I3–K	$3.930(3) \times 2$
In2–In3	$2.9297(9) \times 2$	Sr–In1	$3.497(2) \times 2$
In2–In4	$2.976(2)$	Sr–In1	3.552(3)
In3–In1	$3.095(2)$	Sr–In2	$3.783(2) \times 2$
In3–In2	$2.9297(9) \times 2$	Sr–In3	$3.491(1) \times 4$
In3–In4	$2.977(2)$	Sr–In4	$3.789(2) \times 4$
In4–In1	$3.144(1) \times 2$	Sr–In4	$3.866(2) \times 2$
In4–In2	$2.976(2)$	K–In2	$3.517(2) \times 2$
In4–In3	$2.977(2)$	K–In2	3.575(3)
In4–In4	$2.972(2)$	K–In2	$3.791(3) \times 2$
In1–Sr	3.497(2)	K–In3	3.623(4)
In1–Sr	3.552(3)	K–In3	3.707(4)
In2–Sr	3.783(2)	K–In3	3.930(3)
In3–Sr	3.491(1)	K–In4	$3.502(3) \times 2$
In4–Sr	3.789(2)	K–K	$3.898(6) \times 2$
In4–Sr	3.866(2)		
In2–K	$3.517(2) \times 2$		
In2–K	3.575(3)		
In2–K	$3.791(3) \times 2$		

**EHTB Calculations.** All the calculations were performed with the CAESAR program package developed by Whangbo et al.<sup>21</sup> The atomic orbital energies and exponents for indium contained therein were employed in the calculations ( $H_{ii}$  = orbital energy (eV),  $\zeta$  = Slater exponent): 5s –12.6, 1.903; 5p –6.19, 1.677. The cations were not included particularly because reliable parameters are not available for potassium. Addition of only strontium would certainly bias the results regarding the characteristics of the two distinctive cavities.

**Physical Properties.** The magnetic susceptibilities of the compound were measured between 6 and 296 K on a Quantum Design MPMS superconducting quantum interference device (SQUID) magnetometer at a field of 3T. A quantity of 20.6 mg of powdered K<sub>2</sub>SrIn<sub>7</sub> was loaded into a silica tube in a He-filled glovebox, wherein the sample was held between two tightly fitting silica rods, and the apparatus was sealed under He. The susceptibility data were corrected for the sample holder

(18) *Binary Alloy Phase Diagrams*, 2nd ed.; Massalski, T. B., Ed.; ASM International: Materials Park, OH, 1990; Vol. 3.

(19) TEXSAN for Windows: Crystal Structure Analysis Package; Molecular Structure Corporation: The Woodlands, TX, 1997.

(20) SHELXTL, Bruker AXS, Inc.; Madison, WI, 1997.

(21) Ren, J.; Liang, W.; Whangbo, M.-H. CAESAR for Windows; Prime-Color Software, Inc.: North Carolina State University, Raleigh, NC, 1998.

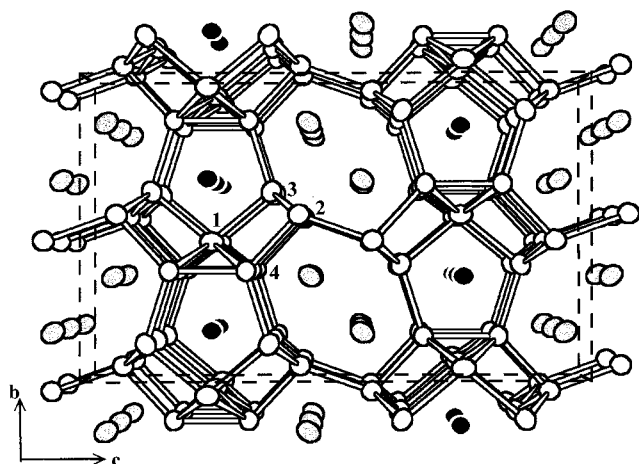


**Figure 1.** [100] view of the orthorhombic cell of  $K_2SrIn_7$  (70% probability displacement ellipsoids). The K, Sr, and In ellipsoids are gray, black, and white, respectively. All atoms lie on mirror planes at  $x = 0$  or  $1/2$  normal to the view.

and the diamagnetic contribution of the atom cores. The corrected molar susceptibility of  $K_2SrIn_7$  is  $-7.1 \times 10^{-5}$  emu mol $^{-1}$  from 296 to 70 K, below which a rapid increase in  $\chi$  is observed. This was attributed to a compositionally minor ferromagnetic impurity judging from the M vs H data.

The electrical resistivities of the phase were measured by the electrodeless "Q" method.<sup>22</sup> A powdered sample of 97 mg was sieved to a 150–250  $\mu\text{m}$  range of grain sizes and diluted with chromatographic  $Al_2O_3$ . The measurements were made at 34 MHz over the range 110–295 K. The resistivities for  $K_2SrIn_7$  fall in the range 11–24  $\mu\Omega\cdot\text{cm}$  and show a small positive temperature coefficient ( $\partial\rho/\rho\partial T$ ) of 0.3% K $^{-1}$ , fairly typical for network structures in this region of the periodic table.<sup>2</sup>

## Results and Discussion

**Structure.**  $K_2SrIn_7$  is the first ternary indide containing mixed cations of different charge types. Its structure can be described as a three-dimensional network of fused indium chains or clusters in which two distinct kinds of channels are occupied separately by potassium and strontium atoms. Figure 1 shows a general [100] view of the unit cell contents for  $K_2SrIn_7$ . All atoms lie on mirror planes at  $x = 0, 1/2$  which are related by C-centering. Distances between neighboring indium atoms fall in a fairly narrow range, 2.930–3.144 Å, and these are all drawn as "bonds". There are four crystallographically different In atoms, among which In1 has six other In neighbors, both In2 and In3 have four each, and In4 has five. All four types make up double zigzag chains or ladders that have common In1 atoms,  $C_{2v}$  symmetry overall, and run along  $\vec{a}$ , Figure 2. One of these is centered around  $x, \sim 0.54, 0.25$  in Figure 1, for example.

The double zigzag chains along  $\vec{a}$  are further stacked head-to-tail along  $\vec{b}$  with the formation of In3–In4 interladder bonds in that direction. Since In2 and In4 differ from In1 and In3 by  $a/2$  in the ladder (Figure 2), this condensation generates parallel columns of pentagonal prisms along  $\vec{b}$  that differ from their two neighbors by  $a/2$  in elevation, i.e., according to the C-centering around the mirror plane at  $z = 0.25$  (and at 0.75 with inversion). An [001] view of this section (white atoms) is shown in Figure 3. This assembly is augmented by In2 atoms (gray) in front and back of the sheet, and these interlink the sheets of pentagonal columns along  $\vec{c}$  via intermediate length In2–In2 bonds about inversion centers,

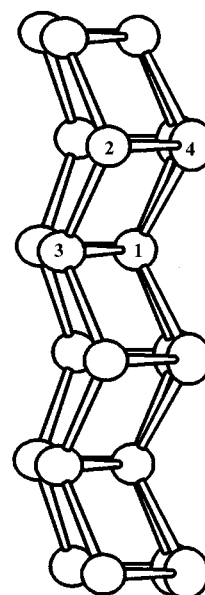


**Figure 2.** An off-[001] view of the condensed pair of zigzag ladders of indium atoms that run along  $\vec{a}$  in  $K_2SrIn_7$ . The chains share In1 atoms. The In4–In4 bonds are eclipsed and not seen.

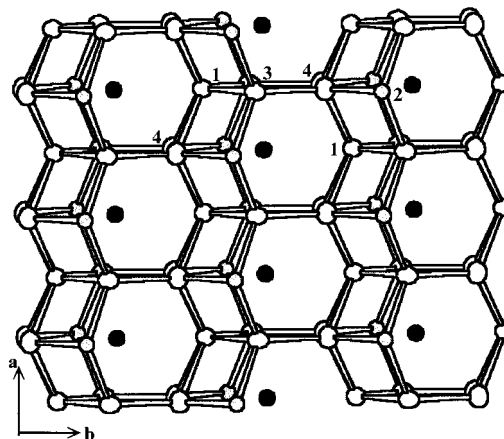


**Figure 3.** A near-[001] section ( $x, y, 1/4$ ) of the sheet of the columns of pentagonal indium prisms (vertical) built of double chains (Figure 2) that share In1 atoms. The gray In2 atoms lie outside of these polyhedral sheets and bond to other sheets along  $\vec{c}$ ; compare Figure 1. Note the 15-atom indium polyhedra that surround the Sr atoms (black).

Figure 1. From another viewpoint, the latter bonds generate layers of ladders around  $x, 1/2, z$ , etc., the aggregation of which along  $\vec{b}$  occurs via In4–In3 and In3–In4 bonds to adjoining layers at the crest and trough of the waves, respectively. The In2–In2 connections involve a weaker bonding mode, however.

The In1 and In4 atoms in these each have more than four bonded neighbors, and so the structure cannot be described in terms of a classical Zintl phase with octet atoms. The distorted trigonal prism of In3 and In4 about In1 can be seen in Figure 3. The distances around In1 are naturally the longest in the structure, and the next longest occur with 5-bonded In4, whereas those with 4-bonded In2 and In3 are shorter and the In2–In3 distance between them is the shortest. The numerical values (Table 3) are typical of those found for both the generally shorter two-center bonds between and the longer polycenter bonding within clusters in other indium systems.<sup>9,23</sup> Meanwhile, cavities in two kinds of channels along  $a$  hold the cations, those between

interlinked puckered eight-membered rings are occupied by pairs of potassium atoms, and those within the condensed pentagonal prisms hold separate strontium atoms (ions). The combination appears to be an efficient means for maximizing the Coulombic portion of the stability of K<sub>2</sub>SrIn<sub>7</sub>. The potassium atoms in the former alternate by  $a/2$  and each has six closer indium neighbors at 3.50–3.62 Å plus, above an arbitrary cutoff, four more indium and a pair of like neighbors at 3.79–3.93 Å. The relatively symmetric cavity about strontium (Figure 3) presents seven cage atoms over 3.49–3.55 Å (In<sub>3</sub> (×4), In<sub>1</sub> (×2), In<sub>1</sub>) plus a second sphere of eight more indium atoms a little more distant at 3.78–3.87 Å (In<sub>4</sub> (×4), In<sub>4</sub> (×2), In<sub>2</sub> (×2)), giving a total coordination number of 15. The average  $d(\text{Sr}-\text{In})$  is 3.664 Å. The pentagons defining the prism are fairly regular, the pair of In<sub>1</sub>–In<sub>3</sub> edges in each being 0.12 Å longer than the other three. On the other hand, the larger pentagon around the waist of Sr (In<sub>4</sub> (×2), In<sub>2</sub> (×2), In<sub>1</sub>) is quite off-center with three contiguous edges of normal length but with the two In<sub>2</sub>–In<sub>1</sub> edges well out of the range of normal bond lengths.

The question has come up as to whether mixtures of nominal K<sup>+</sup> and Sr<sup>2+</sup> might occupy both of the two sites, to the extent that even the closed shell KSr<sub>2</sub>In<sub>7</sub> might be present or possible. None of this appears feasible. The cation cavities in K<sub>2</sub>SrIn<sub>7</sub> seem remarkably and appropriately different. Relative to potassium, the higher charged strontium is fairly symmetrically surrounded by a larger number of framework atoms whereas like neighbors are well removed. Given this consideration and the relatively similar displacement parameters obtained (Table 2) for Sr and K that are 2:1 in scattering power, there seems to be no good reason to believe that a significant mixture of these cations could occur on either site in the net. The difference in their distances to indium (above) are consistent with crystal radii ( $\Delta R = \geq 0.20$  Å at fixed coordination number) if the second spheres of neighbors are included. A much clearer assessment of the true stoichiometry comes from synthetic results. The on-stoichiometry reaction gave  $\geq 90\%$  yield of K<sub>2</sub>SrIn<sub>7</sub> whereas an attempted synthesis of KSr<sub>2</sub>In<sub>7</sub> gave none of this phase (structure) according to the powder pattern.

As explained in the Experimental Section, the phase field of this compound in the ternary system does not appear to be very large, and a sodium substitution gives neither an analogous or any other ternary phase. A variety of related frameworks with double zigzag chains that surround channels can be found in other compounds such as Li<sub>2</sub>Ga<sup>25</sup> and SrIn<sub>4</sub>.<sup>13</sup> The environment around Sr in SrIn<sub>4</sub> is remarkably similar to that in K<sub>2</sub>SrIn<sub>7</sub>, pentagonal prisms with a somewhat more regular pentagon around the waist. The  $d(\text{Sr}-\text{In})$  in SrIn<sub>4</sub> is 0.020 Å less than the value found in the present case. In BaTl<sub>4</sub>, layers of similar stepped, fused pentagonal columns, as shown in Figure 1 around  $x, y, 1/4$ , are condensed together in pairs.

**Electronic Structure.** Understanding the structure of K<sub>2</sub>SrIn<sub>7</sub> is troublesome from the classic viewpoint of Zintl phase behavior. The four crystallographically different In atoms are connected together in a quite complicated In network, in which In<sub>1</sub>, In<sub>2</sub>, In<sub>3</sub>, and In<sub>4</sub> atoms are bonded to six, four, four, and five other indium atoms, respectively. An EH band structure calculation was carried out on the In<sub>7</sub><sup>4-</sup> sublattice in order to better understand the bonding. The densities of states (DOS) and projected partial density of In 5s states (gray) are plotted in Figure 4. The 25 valence electrons present in In<sub>7</sub><sup>4-</sup> fill the orbitals up to a Fermi energy of  $-6.58$  eV, a level which crosses the valence band, so the compound can be termed hypoelec-

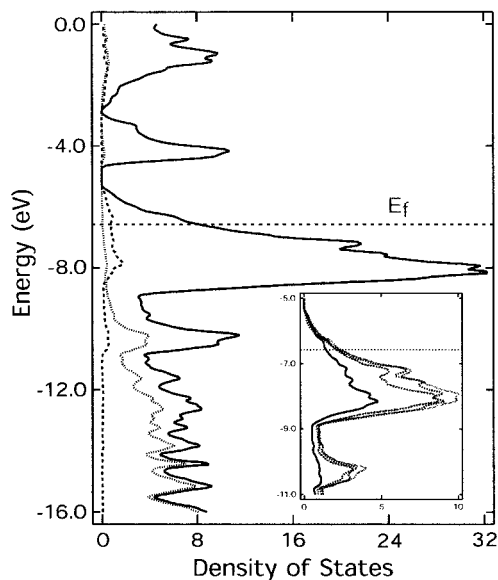


**Figure 4.** Densities of states (DOS) of the anion network of In<sub>7</sub><sup>4-</sup> in K<sub>2</sub>SrIn<sub>7</sub>. Total, solid line; projection of In 5s, gray. The inset shows the partial DOS for, left to right, In<sub>1</sub>, In<sub>4</sub>, In<sub>3</sub>, and In<sub>2</sub>.

tronic. One more electron would completely fill the valence band, and the Fermi level would then fall in a gap  $\sim 0.6$  eV wide (by this admittedly poor approximation). The bands below  $-14.6$  eV involve mainly the s states of In and those located between  $-14.6$  and  $-8.8$  eV consist of mixed s and p bonding states, whereas nearly all bonding from  $-8.8$  eV to above  $E_F$  involves substantially only In p states. The large peak around  $-8$  eV is strongly bonding judging from COOP curves (not shown). The inset in Figure 4 of partial DOS of the four In atoms (ordered, left to right: In<sub>1</sub>, 4, 3, 2) shows that the contributions in this band up toward  $E_F$  are comparable, allowing for the fact that there are half as many In<sub>1</sub> atoms as each of the others. However, at and above  $E_F$ , contributions of the In<sub>1</sub> atoms become relatively dominant. COOP curves show that bonding between all In atoms generally persists to the top of the valence band.

The In<sub>1</sub> states that fall above  $E_F$  are found to be particularly concentrated in the contributions of its p<sub>z</sub> orbital, as shown in Figure 5, whereas its p<sub>x</sub> and p<sub>y</sub> orbitals are relatively uninvolved. Around In<sub>1</sub> only In<sub>1</sub>–In<sub>3</sub> bonding is important in this region. Recall that the p<sub>z</sub> orbital on In<sub>1</sub> lies normal in Figure 3. It thus appears that the weakest bonding states in K<sub>2</sub>SrIn<sub>7</sub>, those about the multicenter In<sub>1</sub>, are simply left empty when the structure and  $E_F$  are fixed by the strong Coulombic contributions and the four-electron limit available from the cations therein. A trivalent ion substitution for Sr may be possible without a change in structure. Related and somewhat similar bonding features have been found in our recent studies of SrIn<sub>4</sub> and Sr<sub>3</sub>In<sub>5</sub> wherein one-electron deficiencies reside at the longest and weakest In–In bond and in an approximately nonbonding orbital of the least bonding In atom, respectively.<sup>13,14</sup>

The observed properties of K<sub>2</sub>SrIn<sub>7</sub> (Experimental Section,  $\geq 90\%$ ) provide some support as well as novelty regarding these electronic considerations. The fairly low resistivity,  $\rho_{(296)} \sim 24$   $\mu\Omega\cdot\text{cm}$ , and its positive temperature coefficient ( $0.3\%$  K<sup>-1</sup>) are in accord with the open band and the presumed presence of free carriers. (It is unlikely that  $\leq 10\%$  of an unknown metallic impurity in a semiconducting matrix would give resistivities this low.) On the other hand, the small temperature-independent diamagnetic susceptibilities observed,  $\chi_M \sim -7.1 \times 10^{-5}$  emu $\cdot\text{mol}^{-1}$  over 160–296 K, appear to reflect a common

(24) Sevov, S. C.; Corbett, J. D. *Z. Anorg. Allg. Chem.* **1993**, 619, 128.

(25) Müller, W.; Stöhr, J. *Z. Naturforsch.* **1977**, 32B, 631.

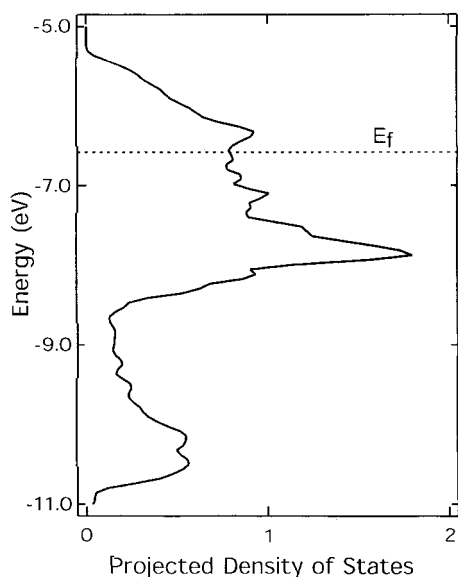


**Figure 5.** Projection of the partial density of states for the  $p_z$  orbital on In1.

property of not only elements in this region of the periodic table but also of many of their compounds with the active metals. Indium metal itself presents remarkably similar contradictions ( $\rho_{295} = 8.75 \mu\Omega\cdot\text{cm}$ , changing by 0.39%  $\text{K}^{-1}$ ;  $\chi_{\text{rt}} = -6.4 \times 10^{-5} \text{ emu}\cdot\text{mol}^{-1}$ ). We have earlier observed that many alkali-metal compounds of polyanionic indium (as well as of thallium

clusters and networks) often exhibit fairly low metal-like conductivities, even with apparently closed band or MO states, but with characteristic diamagnetic properties.<sup>28,29</sup> The chain compound  $\text{Cs}_5\text{Cd}_2\text{Tl}_{11}$  is a more recent example.<sup>17</sup> The seeming susceptibility contradiction is usually attributed to the wide bands and large atomic orbitals present and thence to the low effective  $m_e$  values. These lead to diamagnetic Landau terms that outweigh the Pauli contributions as well as to enhanced electron mobilities.<sup>30</sup>

**Acknowledgment.** We thank D.-K. Seo for helpful discussions and J. Ostenson for measurement of the magnetic susceptibility data.

**Note Added in Proof:** Attempts to substitute La or Y (R) for Sr to give a closed-shell product instead produce mainly the more stable  $\text{RIn}_3 + \text{KIn}_4$ .<sup>31</sup>

**Supporting Information Available:** Tables of additional crystallographic and refinement parameters. This material is available free of charge via the Internet at <http://pubs.acs.org>.

IC010023U

(26) *Am. Inst. Phys. Handbook*, 3rd ed., 1972.

(27) *Handbook of Chemistry and Physics*, 65th ed.; CRC Press: Boca Raton, FL, 1984; p E108.

(28) Reference 2, p 172.

(29) Reference 3, p 686.

(30) Elliott, S. *The Physics and Chemistry of Solids*; John Wiley & Sons: Chichester, U.K., 1998.

(31) Li, B.; Corbett, J. D. Unpublished research, 2001.